Journal of Catalysis **184,** 316–326 (1999)
Article ID jcat.1999.2428, available online at http://www.idealibrary.com on IDEAL®

Cu/SiO_2 and Cu/SiO_2–TiO_2 Catalysts

I. TEM, DR UV-Vis-NIR, and FTIR Characterisation

F. Boccuzzi,*,[1] S. Coluccia,* G. Martra,* and N. Ravasio†

*Dipartimento di Chimica I.F.M., Università di Torino, via P. Giuria 7, I-10125 Turin, Italy; and †C.N.R. CSSCMTBO, c/o Dipartimento di Chimica I.M.A., via Venezian 21, I-20133 Milan, Italy

Received July 31, 1998; revised December 13, 1998; accepted January 13, 1999

Three 8 wt% copper catalysts supported on SiO_2 and on two SiO_2/TiO_2 powders with different TiO_2 content have been prepared by a "chemisorption–hydrolysis" method. Transmission electron microscopy indicated that after calcination the three catalysts contain supported particles which are small and quite homogeneous in size (mean diameter, $d_m = 3.0$ nm). These particles slightly increase in size after reduction in H_2 up to 773 K ($d_m = 3.5$ nm). On the basis of the diffuse reflectance UV-Vis-NIR spectra CuO and Cu_2O were found to be present after calcination, while the electronic spectra were dominated by the features due to metallic Cu particles already after a mild reduction in H_2 at 523 K. FTIR spectra of CO adsorbed onto the three catalysts reduced at 523 K appeared very similar. By a spectral fitting procedure, four different carbonylic species were evidenced, three assigned to carbonylic adducts on different types of microfacets exposed at the surface of three-dimensional Cu particles and one related to CO molecules adsorbed on plate-like two-dimensional copper particles. By increasing the reduction temperature an overall decrease in intensity of the bands due to CO adsorbed on copper supported on silica–titania carriers was observed, probably because of the formation of titanium suboxides that can cover a fraction of the copper sites. Furthermore, the CO–O_2 and CO–NO reactions were studied by FTIR spectroscopy of the adsorbed species and quadrupole mass analysis of the gas phase over the catalysts. This allows the elucidation of the nature of the surface sites involved in the activation of these molecules and the nature of the intermediates present at the surface of the catalysts during the reactions. The role played in these reactions by the uncoordinated copper surface atoms exposed at the surface of the two different types of Cu particles will be discussed.

Key Words: **Cu catalysts supported on different carrier; TEM; DR UV-Vis-NIR characterisation; FTIR spectroscopy of adsorbed CO; CO–O_2 and CO–NO reactions.**

1. INTRODUCTION

Over the past few decades it has been observed by many authors that catalytic performances of metal catalysts are strongly dependent on the support, on the preparation method, and on the catalyst activation (1–3). In this respect, copper particles dispersed on semiconductor oxides, such as ZnO and TiO_2, by different methods have been previously characterised by some of us (4–7). More recently, we have studied two kinds of Cu/TiO_2 samples, one obtained by wet impregnation and the other by the so-called "chemisorption–hydrolysis" method (8). It was shown that after a mild reduction the last one is the most active in promoting CO–O_2, CO–NO, and hydrogenation of dienes reactions. The analysis of structural and spectroscopic data showed that on the samples prepared by chemisorption–hydrolysis the active sites for CO oxidation at room temperature are Cu centres exposed at the surface of small and well-dispersed three-dimensional (3D) copper metallic particles. These sites disappear by increasing the reduction temperature, probably owing to the formation of TiO_x phases ($x < 2$), covering almost completely the 3D copper particles. On both Cu/TiO_2 samples two-dimensional (2D) Cu small particles, rendered electropositive by the interaction with the oxidic support, have been put in evidence (6). Moreover, these particles were found to be the only present at the surface of the wet impregnated samples.

As for copper catalysts supported on insulating oxides, an increase in the CO–NO activity was observed by increasing the reduction temperature on Cu/SiO_2 samples prepared by the homogeneous deposition of copper ions onto the surface of suspended silica using the decomposition of urea at 363 K (9). On these samples an incomplete copper reduction at the lower activation temperature probably occurred; therefore, the increase in the activity observed by increasing the reduction temperature can be ascribed to an increase in the exposed metallic area. However, as for Cu/TiO_2 samples, the properties of the copper supported on silica can be strongly dependent on the preparation method also. This fact will appear evident by a comparison of our experimental data with those previously reported by Balkenende *et al.* (9).

In this paper we will present also experimental data concerning the CO oxidation, the CO–$^{18}O_2$ scrambling

[1] To whom correspondence should be addressed.

0021-9517/99 $30.00

reaction, and the CO–NO reaction. The oxidation of carbon monoxide constitutes an important step in many relevant processes such as methanol synthesis, water–gas shift reaction, and automotive exhaust controls. Some studies have shown that over copper-based catalysts methanol synthesis is likely to occur through the hydrogenation of carbon dioxide produced by the reaction between carbon monoxide and oxygen, while in the water–gas shift reaction carbon monoxide removes surface hydroxyl or oxygen species produced by the dissociation of water.

Recently, copper has also been tested as a possible substitute for palladium and platinum for the reduction of nitrogen oxides by carbon monoxide in automotive catalytic converters. Even though the importance of carbon monoxide oxidation has been recognised, a full understanding of this reaction has not been achieved, in particular for the role of the oxidation state of the metals, for their coordinative unsaturations, and for the contribution of the support.

As far as the role of the oxidation state of the metal is concerned, Jernigan and Somorjai (10) recently discussed CO oxidation over Cu, Cu_2O, and CuO and showed that the rate of the reaction decreased with increasing copper oxidation state. However, also the other two points, the coordinative unsaturations of these sites and the nature of the support, can play a significant role.

Often the best catalysts are more complex than a binary system formed by one supported phase dispersed on a monocomponent carrier. For instance, a lot of interest has been recently devoted to the use of mixed SiO_2–TiO_2 systems as support; they are appearing very attractive to improve the mechanical strength, thermal stability, and surface area of TiO_2. Moreover, these mixed oxides exhibit also interesting properties related to the generation of new catalytic sites for selective oxidation reactions such as cyclohexene epoxidation (11). Even more attractive would be to combine the catalytic effect of such materials with that of a metallic phase to design new bifunctional catalysts.

In this paper we will present a characterisation by different techniques of three 8 wt% copper catalysts supported on SiO_2 and on two SiO_2–TiO_2 powders with different TiO_2 content, prepared by a method that, for the sake of uniformity with previous papers, we continue to call chemisorption–hydrolysis (6, 7, 8). The effect of reducing pretreatments and a study of the CO–O_2 and CO–NO reactions will be described. In the next paper (Part II) the catalytic behaviour of these systems in the polymerisation by oxidative coupling of 2,6-dimethyl phenol will be discussed.

2. EXPERIMENTAL

2.1. Materials

Cu/SiO_2, Cu/SiO_2–0.3%TiO_2, and Cu/SiO_2–2.3%TiO_2 catalysts, hereafter referred to as Cu/Si, Cu/SiTi0.3, and Cu/SiTi2.3, were prepared by what was called in previous papers (6, 7, 8) chemisorption–hydrolysis. The support was added to a $Cu(NH_3)_4^{2+}$ solution prepared by adding NH_4OH to a $Cu(NO_3)_2 \cdot 3H_2O$ solution until pH 9. After 20 min under stirring, the slurry, held in an ice bath at 273 K, was slowly diluted in order to allow hydrolysis of the copper complex and deposition of the finely dispersed product to occur. Under these conditions, no dissolution of silica was detected. The solid was separated by filtration, washed with water, dried overnight at 383 K, and calcined in air at 673 K for 4 h. In all cases the Cu content was ca. 8 wt% (Table 1). Other relevant surface and textural properties of the samples, metallic and BET specific surface area, pore volume, and size are listed in Table 1.

TABLE 1

Relevant Surface and Textural Properties of the Samples: Specific Surface Area (SSA_{BET}), Pore Volume (PV), Metal Loading (Cu wt%), and Metallic Specific Surface Area ($S_{Cu(0)}$)

Catalyst	SSA_{BET} ($m^2 \cdot g_{Cu}^{-1}$)	PV ($ml \cdot g^{-1}$)	Cu (wt%)	$S_{Cu(0)}$ ($m^2 \cdot g_{Cu}^{-1}$)
SiO_2	320	1.75	—	—
Cu/Si	263	0.78	7.68	129
$SiO_2/TiO_2$0.3	330	1.90	—	—
Cu/SiTi0.3	352	0.94	8.85	138
$SiO_2/TiO_2$2.3	340	1.20	—	—
Cu/SiTi2.3	349	1.01	8.10	120

High purity gases (Matheson) were employed in the activation treatments and in the adsorption and reaction experiment. In particular, O_2, H_2, and CO were used without any further purification, whilst NO was freshly distilled before use and its purity checked by mass analysis.

2.2. Methods

The Cu(0) surface area was determined by the N_2O dissociative adsorption method (12, 13), using a pulse-flow technique. The Cu(0) surface area was computed by considering a surface coverage factor (moles of oxygen atoms per moles of surface Cu(0) atoms) $Q = 0.35$ and a mean surface area for a copper site of 7.41 Å (14).

Electron micrographs of the samples were obtained by a Jeol 2000EX microscope equipped with a polar piece and top entry stage. Before the introduction in the instrument, the samples, in the form of powders, were ultrasonically dispersed in isopropyl alcohol, and a drop of the suspension was deposited on a copper grid covered with a lacey carbon film. Histograms of the particle size distribution were obtained by counting onto the micrographs at least 300 particles, and the mean particle diameter (d_m) was calculated by using the formula $d_m = \sum d_i n_i / \sum n_i$, where n_i was the number of particles of diameter d_i.

Diffuse reflectance UV-Vis-NIR measurements were performed with a Varian CARY5 spectrometer equipped

with a diffuse reflectance sphere. The measured reflectances are relative to a $BaSO_4$ standard and were converted in the Schuster–Kubelka–Munk function $F(R_\infty)$. The samples were introduced in a suitable reflectance cell which allowed all thermal treatments to be carried out in a controlled atmosphere.

The IR spectra (2 cm^{-1} resolution) were recorded at room temperature (RT) in an infrared cell designed to treat the samples *in situ*, using a Perkin–Elmer FTIR 1760 instrument.

The $CO–O_2$ and CO–NO reaction features were monitored by FTIR spectroscopy by recording spectra at increasing times of contact. At the same time the IR cell was permanently connected through a needle valve to a VG Micromass 100 mass spectrometer to obtain the analysis of the gas phase during the reaction. Due to the very low flow rate, the overall gas pressure was not significantly modified during the experiment.

2.3. Samples Pretreatments

The samples were first submitted to a preliminary pretreatment in oxygen at 673 K, then reduced in H_2 at 523 K and 773 K, and outgassed at the same temperature.

3. RESULTS AND DISCUSSION

3.1. TEM Characterisation

In Fig. 1 TEM images of the Cu/Si catalyst calcined at 673 K (Fig. 1a) and then reduced at 773 K (Fig. 1b) are shown. In both cases small particles well distributed onto the silica carrier are observed. On the basis of the UV-Vis-NIR results (vide infra) they should correspond to CuO and Cu_2O phases for the calcined sample and to a Cu(0) phase for the reduced one.

A statistical analysis of the dimension of the particles present after calcination resulted in a quite narrow size distribution over the 2.0–5.5 nm range and in a mean diameter $d_m = 3.0$ nm (Fig. 2a). For the reduced sample, particle sizes are distributed essentially over the same range, but a slightly larger mean diameter $d_m = 3.5$ nm was obtained (Fig. 2b). This indicates that a slight growth of the supported particles occurred during the reduction treatment at 523 K. Noticeably, on the basis of the mean diameter $d_m = 3.5$ nm and assuming that Cu particles are spherical, a specific surface area of the metallic copper phase $S_{Cu(0)} = 112\ m^2 \cdot g^{-1}$ was calculated, in good agreement with the value obtained by the N_2O dissociative adsorption method (Table 1).

TEM investigations were also carried out on the Cu/SiTi0.3 and Cu/SiTi2.3 catalysts. A striking similarity between these last and the Cu/Si system was observed. In fact, the supported particles on both the silica–titania carriers exhibit the same particle size distribution and the same mean diameter (see Table 2) than for the Cu/Si catalyst, both in the oxidised and in the reduced forms.

TABLE 2

Mean Diameter (d_m) of the Supported Particles Observed by TEM on the Catalysts Calcined at 673 K and Reduced at 523 and 773 K

Catalysts	Calcined samples d_m (nm)	Reduced samples[a] d_m (nm)
Cu/Si	3.0	3.5
Cu/SiTi0.3	3.0	3.4
Cu/SiTi2.3	3.2	3.5

[a] The same values of d_m of the supported particles were obtained after reduction of the samples both at 523 and 773 K.

3.2. Diffuse Reflectance UV-Vis-NIR Spectroscopy

All catalysts were characterised by diffuse reflectance UV-Vis-NIR spectroscopy at different stages of the activation procedure. Moreover, the spectra of the bare supports were recorded also (Fig. 3a). Both the silica–titania carriers (Fig. 3a, curves 2 and 3) exhibit a main band in the 35,000–25,000 cm^{-1} range, where the valence to conduction transition edge of bulk TiO_2 is observed (see the spectrum of a pure titania powder reported for the sake of comparison, in Fig. 3a, curve 1). However, a close inspection of these samples by electron microscopy did not evidence the presence of TiO_2 particles. This feature suggests that the titania phase should be highly dispersed onto the silica. Noticeably, the formation of a very thin amorphous layer of TiO_2 on SiO_2 was recently reported (10c). Differences in the shape of the absorptions observed for the $SiO_2–TiO_2$ carriers with respect to the TiO_2 powders could be due to the different morphologies of the titania phases in the two cases.

Additional adsorptions at 13,500 cm^{-1} and in the 20,000–30,000 cm^{-1} range were observed in the spectra of the calcined catalysts (Fig. 3b), due to the supported phase. The close similarity in position, shape, and intensity of these additional features for the three catalysts (all loaded with almost the same copper amount) indicates that they contain the same types of supported copper species. As for the assignment of these absorptions, the band at 13,500 cm^{-1} should be due to the fundamental transition of CuO small particles, blue shifted with respect to the bulk transition (occurring at 11,500 cm^{-1}) as a consequence of the small size of the particles; a similar effect has been observed in the optical spectra of different nanocrystalline semiconductors such as ZnO and CdS (15). The assignment of the absorption in the 20,000–30,000 cm^{-1} range is more difficult.However, Cu_2O layers on a copper substrate were found to exhibit a maximum of absorption at ca. 20,000 cm^{-1} (16), and then the component observed in the 20,000–30,000 cm^{-1} region could be tentatively assigned to Cu_2O layer-like species.

After reductive treatments at 523 and 773 K a strong absorption with a maximum at 18,000 cm^{-1} grows up in all

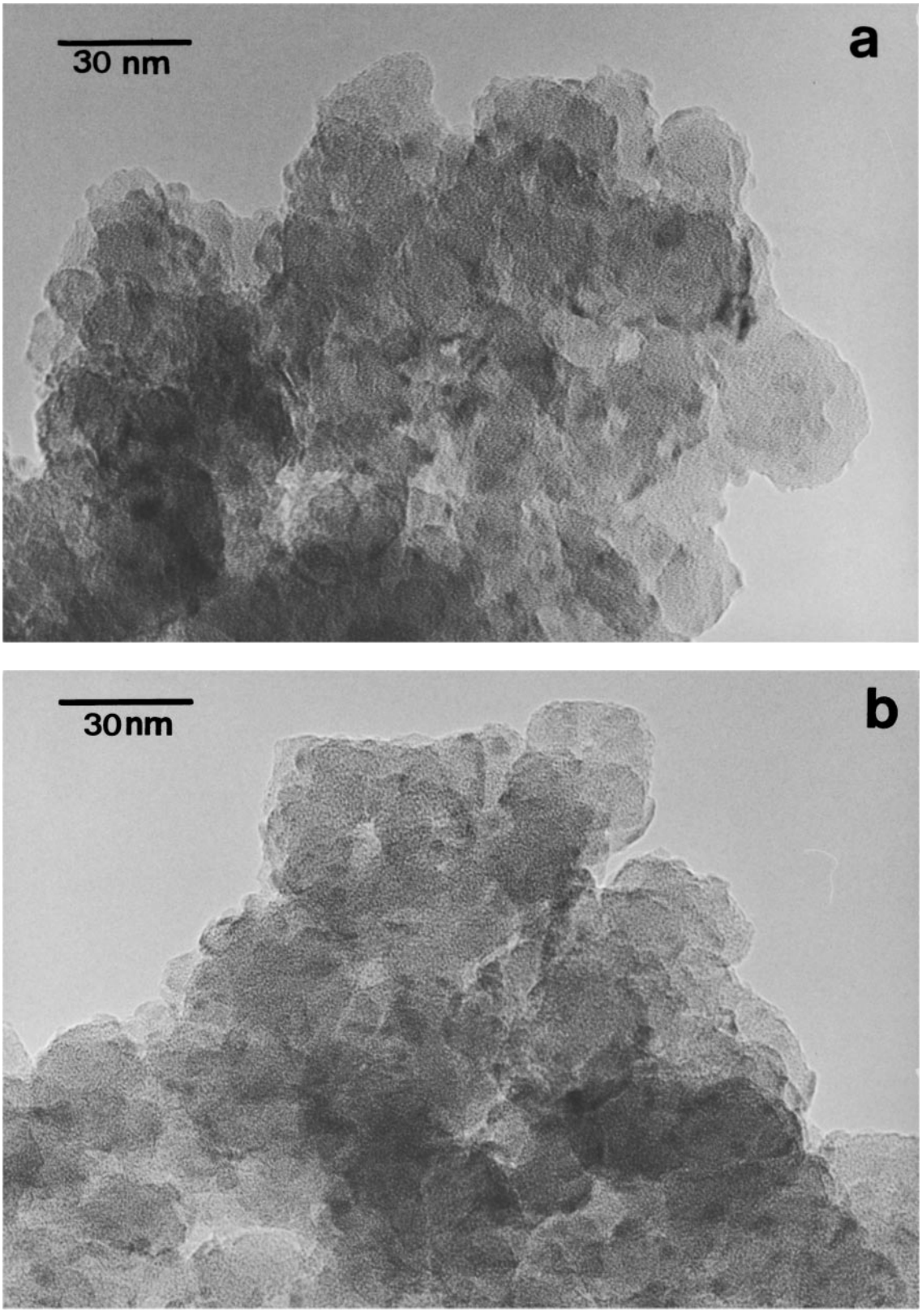

FIG. 1. Electron micrographs of the Cu/Si catalyst: (a) after calcination at 673 K and (b) after reduction at 773 K. Original magnification: ×200,000.

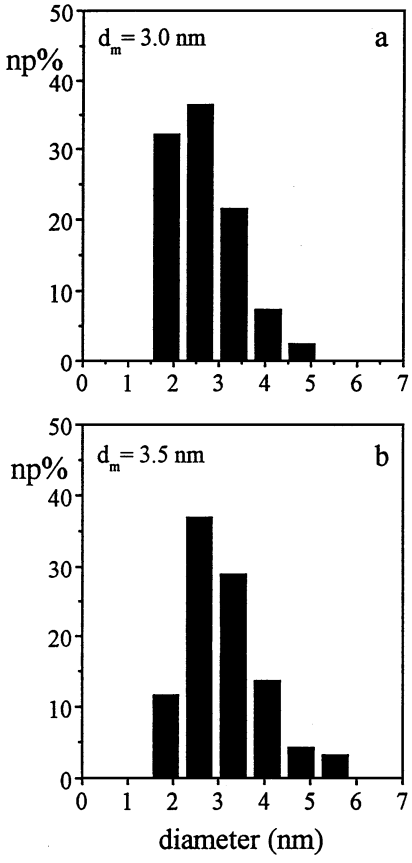

FIG. 2. Size distribution of the supported particles present in the Cu/Si catalyst: (a) after calcination at 673 K and (b) after reduction at 773 K.

the samples containing silica, with a very similar intensity and shape (Fig. 3c). The strong absorption at 18,000 cm^{-1} can be assigned to the plasmonic absorption of metallic copper particles produced by reduction.

3.3. FTIR Spectroscopic Features of CO Adsorbed on the Surface Sites of Cu/SiO_2 and Cu/SiO_2–TiO_2 Samples

Figure 4a reports the FTIR spectra in the carbonylic region of CO adsorbed at full (10 mbar) and decreasing coverages on the Cu/Si sample reduced and outgassed at 523 K. The spectra exhibit a main peak at 2100 cm^{-1} with an evident shoulder at 2130 cm^{-1} and a weaker one at 2070 cm^{-1}. Upon decreasing the CO pressure a gradual decrease in intensity of all the components is observed (Fig. 4a, curves 1–9). All these spectra can be well fitted by the superposition of four lorentzian bands. An example is shown in Fig. 4b, where the experimental spectrum at full CO coverage is compared with the curvefitting resulting from the addition of four individual components. The integrated intensity of these four components at the various CO coverages was reported versus their position in frequency, obtaining the diagrams shown in Fig. 4c. It appears evident that

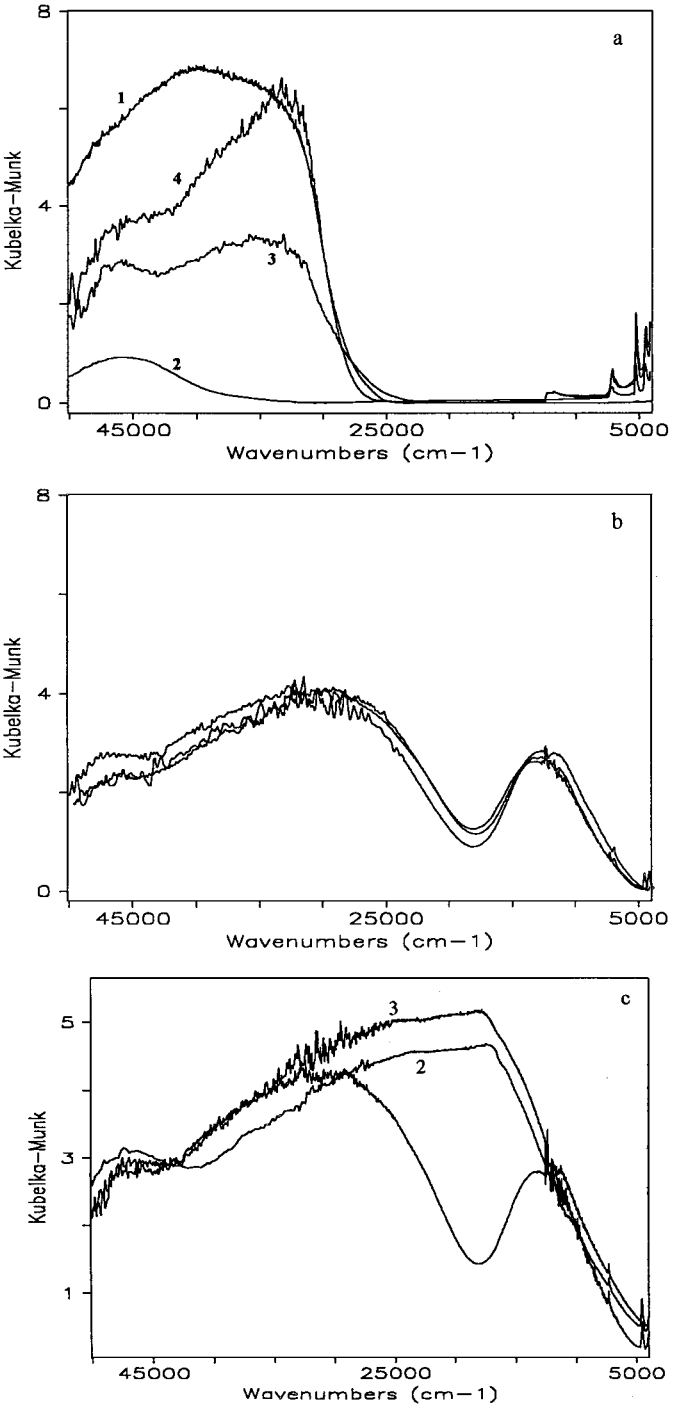

FIG. 3. Diffuse reflectance UV-Vis-NIR spectra of the bare supports (a) and of the Cu/Si, Cu/SiTi0.3, and Cu/SiTi2.3 samples in the calcined (b) and reduced (c) forms. (a) Spectra of the bare carriers outgassed and oxidised (100 Torr O_2) at 673 K: (1) TiO_2 P25 powders, reported for the sake of comparison; (2) SiO_2; (3) SiO_2–TiO_2 0.3 wt% TiO_2; (4) SiO_2–TiO_2 2.3 wt% TiO_2. (b) Spectra of the Cu containing catalysts calcined in air at 673 K: (1) Cu/Si; (2) Cu/SiTi0.3; (3) Cu/SiTi2.3. (c) Spectra of the Cu/Si catalyst: (1) after calcination at 673 K (the same as curve 1 in b); (2) after reduction in 30 mbar H_2 at 523 K; (3) after reduction in 30 mbar H_2 at 773 K.

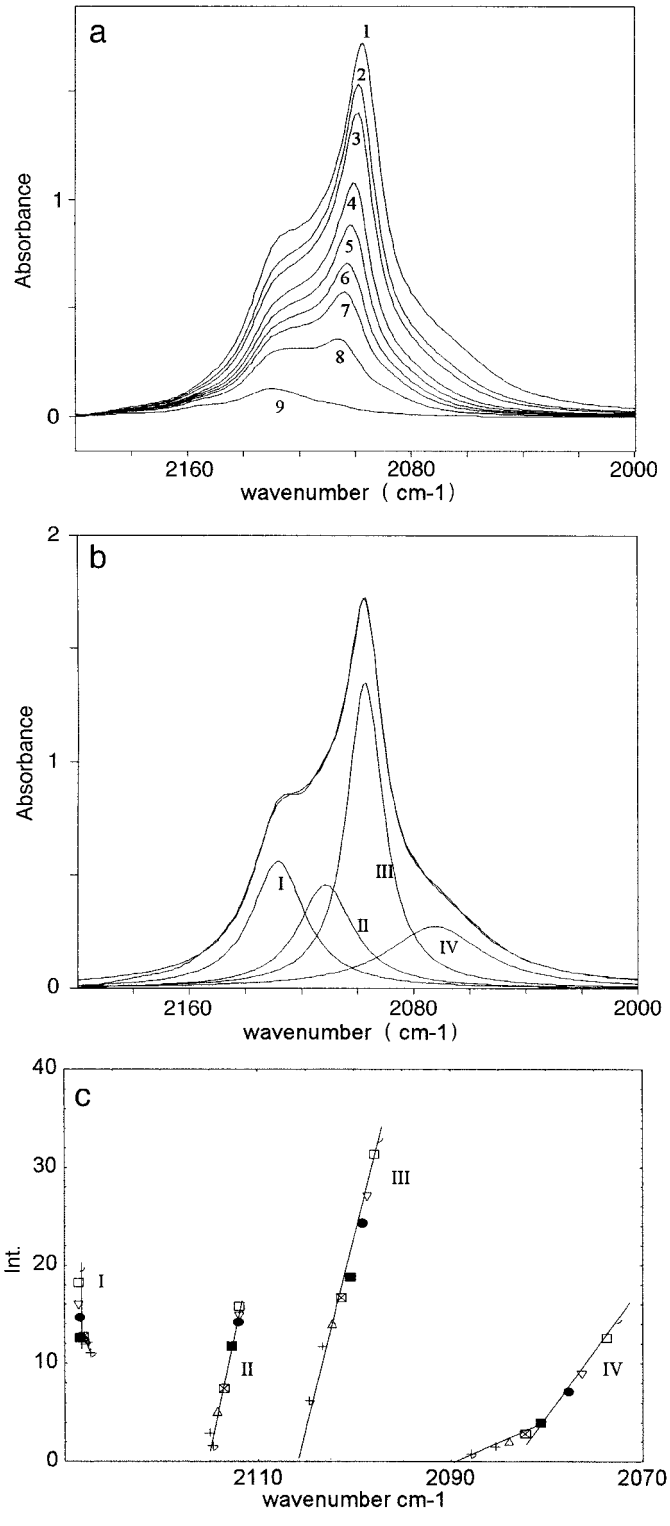

FIG. 4. FTIR spectra of the carbonylic region of CO adsorbed on the Cu/Si reduced in 30 mbar H_2 for 45 min at 523 K and then outgassed for 45 min at the same temperature. (a) Spectra at decreasing coverages, from (1) the presence of 10 mbar CO, to (9) after outgassing 10 min at room temperature. (b) Curvefit of curve 1 in (a) obtained by the addition of the four Lorentzian bands shown in the layer. (c) Integrated intensities vs frequency at maximum of the four components used to fit the experimental curves in (a) (curve fitting procedure carried out without fixed parameters).

component I reduces its intensity without frequency shift, whereas the decrease in intensity of components II and II′ is accompanied by a blue shift of their maximum position.

On the basis of the close similarity with the spectra of CO adsorbed on the Cu/TiO_2 sample prepared by the same method discussed in a previous work (6) and by comparison with the spectra of CO adsorbed on well-defined monocrystalline surfaces reported in the literature (17), components II and III can be assigned to CO adsorbed on Cu stepped surfaces and on small (111) microfacets, respectively. Band II′, close in frequency to component II, can be tentatively assigned to CO adsorbed on a different high index plane. These features indicate that different types of microfacets are exposed at the surface of the three-dimensional Cu particles.

As fully discussed in the paper devoted to the Cu/TiO_2 sample (6) component I may correspond to CO adsorbed on small two-dimensional copper particles rendered partially electropositive by the interaction with the oxygen atoms at the surface of the carrier, which are able to withdraw electron density from the metal phase. Evidences of electropositivised thin metallic particles supported on oxides have been recently reviewed by Campbell (18). The position in frequency of this component appears very close to that observed for CO adsorbed on Cu(I) copper sites (9). However, the adsorption of CO on these centres is known to be partly irreversible at room temperature (9), whereas in the present case the 2128 cm^{-1} component is almost completely depleted by briefly outgassing at RT (Fig. 4, curve 9), as for CO stabilised on Cu metal sites (9). This behaviour suggests that, although positivised, the Cu centres at the surface of 2D particles still keep a metal character.

All the components in the carbonylic spectra should then correspond to CO molecules stabilised on metallic copper sites, indicating that the reduction of the supported Cu particles is accomplished in the mild activation condition adopted (reduction in 30 mbar H_2 at 523 K for 45 min). Interestingly, Cu/SiO_2 catalysts prepared by homogeneous deposition of copper ions onto the surface of suspended silica by using the decomposition of urea and then calcined at 673 K were reported to be fully reduced only after treatment in 10% H_2/Ar at 873 K for 16 h (9a). This striking difference in reducibility with respect to the Cu/SiO_2 sample object of the present paper should be due to the different preparation method adopted in the two cases. In particular, the copper hydrosilicate crisocolla was identified as the precursor of the metal phase in both the dried and calcined forms of those samples, whereas no copper oxides were detected (9b). The reduction of such a hydrosilicate phase should require higher temperatures to obtain metallic copper particles.

The adsorption of CO on Cu/SiTi0.3 and Cu/SiTi2.3 samples reduced and outgassed at 523 K produced carbonylic spectra very similar to those obtained for the Cu/Si system (spectra not reported for the sake of brevity). Also in

these cases, the best curfitting of the experimental spectra at decreasing coverage was obtained by introducing four Lorentzian components located at the same frequency as those found for the Cu/Si sample. This indicates that, for this reduction treatment, the surface features of the Cu particles are not affected by the presence of the titania phase onto the carrier.

The same four components were also found by fitting the experimental spectra of CO adsorbed on all the three samples reduced and outgassed at 773 K. This feature confirms that the reduction of the Cu phase is already accomplished by treating in H_2 at 523 K. In fact, an increase of the extent of reduction of the copper phase should be accompanied by a shift to a lower frequency of the band due to adsorbed CO (9), whereas this behaviour did not occur in the present case.

By comparing the values of the integrated intensity of each of these components for the samples activated at 523 and 773 K (Table 3), it appears evident that by increasing the reduction temperature the components at 2110, 2100, and 2070 cm^{-1} grow up in the case of the Cu/Si system, while these absorptions decrease in intensity for the Cu/SiTi0.3 and Cu/SiTi2.3 samples. In all cases by increasing the activation temperature a depletion of the 2128 cm^{-1} component is observed, although in a larger extent for the catalysts supported on silica–titania.

Electron microscopy clearly indicated that the size of the copper particles does not significantly change by increasing the reduction temperature, and then it can be inferred that the observed evolution of the integrated intensity of the various spectral components is not due to relevant modifications of the morphology and the dispersion of the Cu phase (e.g., sintering of the metal particles in the case of the samples supported on silica–titania). The increase in intensity of the 2128, 2110, and 2070 cm^{-1} components observed by passing from the Cu/Si activated at 523 K to that reduced at 773 K could be then due to the fact that at lower outgassing temperature the silica surface is still widely hydroxylated, and therefore some of the Cu sites at the boundary between the metal particles and the support could be overcrowded by silica surface −OH groups. By increasing the outgassing temperature a large fraction of such hydroxyl groups is desorbed, and then a larger amount of Cu sites is available to adsorb CO.

The lower intensity of the bands due to CO adsorbed on the Cu/SiTi0.3 and Cu/SiTi2.3 samples reduced at 773 K with respect to those observed in the case of the samples reduced at 523 K is probably related with the reduction of titanium oxide leading to the defective suboxide of titania, covering a fraction of the copper sites. A similar effect, although more pronounced, was observed in the case of the Cu/TiO_2 catalyst (6).

3.4. *Effects of Oxidative Interactions on Preadsorbed CO*

3.4.1. CO–O_2 interaction. Curve 1 in Fig. 5a is the spectrum of CO adsorbed at full coverage on the Cu/Si catalyst. The admission of $^{16}O_2$ causes the disappearance of the two components at 2103 and 2070 cm^{-1} in few minutes; at the same time the shoulder at 2128 cm^{-1} intensifies and appears more structured (Fig. 5a, curves 2). At longer reaction times three overlapped components, at 2116, 2128, and 2138 cm^{-1} become evident and an additional absorption appears at 2146 cm^{-1} (Fig. 5a, curves 3, 4). Parallel experiments indicated that these four components are partially irreversible by outgassing at RT (spectra not shown for the sake of brevity). Moreover, a very weak absorption at 2350 cm^{-1} assigned to CO_2 is also detected. By further increasing the contact time the component at 2146 cm^{-1} is completely depleted and the absorptions in the 2116–2138 cm^{-1} frequency range are reduced in intensity (Fig. 5a, curve 5). The immediate decrease in intensity by O_2 admission of the bands at 2103 and 2070 cm^{-1}, assigned to CO adsorbed on 3D copper particles, indicates that copper sites exposed at the surface of 3D particles are highly reactive towards oxygen. As will be shown in the next paper, sites exposed at the surface of the 2D particles were found less reactive towards O_2. This difference in reactivity is probably related

TABLE 3

Integrated Intensity (I/M, Normalised to the Weight of the Pellet) of the Four Components at 2128, 2110, 2100, and 2070 cm^{-1} Obtained by Fitting the FTIR Spectra of CO (10 mbar) Adsorbed onto the Catalysts Reduced at 523 and 773 K

		Band at 2128 cm^{-1}		Band at 2110 cm^{-1}		Band at 2100 cm^{-1}		Band at 2070 cm^{-1}	
Catalysts	T reduction (K)	I/M (cm^{-1})	$\Delta I/M\%$[a]	I/M (cm^{-1})	$\Delta I/M\%$[a]	I/M (cm^{-1})	$\Delta I/M\%$[a]	I/M (cm^{-1})	$\Delta I/M\%$[a]
Cu/Si	523	16		17		38		14	
	773	13	−14	21	+23	50	+31	17	+19
Cu/SiTi0.3	523	18		26		48		16	
	773	5	−72	10	−61	27	−61	7	−54
Cu/SiTi2.3	523	16		16		35		14	
	773	5	−69	8	−50	34	−2	9	−32

[a] $\Delta I/M\% = [(I/M_{\text{red 773}} - I/M_{\text{red 523}})/I/M_{\text{red 523}}] \times 100$.

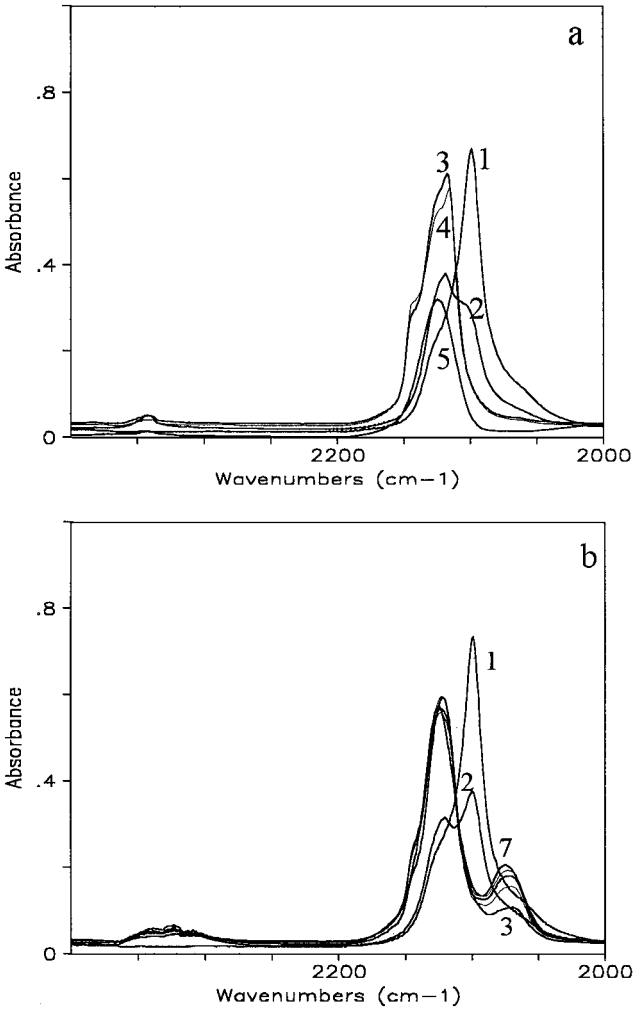

FIG. 5. FTIR spectra of O_2 interaction with CO preadsorbed on Cu/Si reduced and outgassed at 523 K. (a) (1) Spectrum recorded in the presence of 10 mbar CO; (2–5) spectra recorded 2, 4, 8, and 30 min, respectively, after the inlet of 10 mbar $^{16}O_2$ into the cell already containing 10 mbar CO. (b) (1) Spectrum recorded in the presence of 10 mbar CO; (2–7) spectra recorded 2, 4, 6, 8, 10, and 30 min, respectively, after the admission of 10 mbar $^{18}O_2$ onto preadsorbed CO.

to the fact that flat particles are rendered electropositive by the interaction with the support and therefore the Cu–CO bond is stronger and the copper atoms are less oxophilic. The 2146 cm^{-1} band, certainly due to a carbonyl species adsorbed on an oxidised copper site, can be tentatively assigned to CO stabilised on copper centres interacting with a couple of oxygen atoms deriving from the dissociation of the O_2 molecule. In fact, it must be considered that this band was not observed by using NO as an oxidant (see infra), the dissociation of which on the copper surface produces isolated oxygen atoms.

The same experiment was carried out by using $^{18}O_2$ (Fig. 5b). The interaction of adsorbed CO with these molecules produces peaks in the 2116–2140 cm^{-1} range, broader and less structured than in the case of the $^{16}O_2$. Furthermore, an additional band at 2060–2080 cm^{-1} is detected. This last absorption is red shifted by 48–50 cm^{-1} in comparison with the bands at 2116 and 2128 cm^{-1} and similar to these components, appeared partially irreversible to the outgassing at room temperature (spectra not shown for the sake of brevity). On the basis of both these features the 2060–2080 cm^{-1} band can be assigned to $C^{18}O$ molecular species adsorbed on oxidised copper sites. This assignment is also supported by the quadrupole mass analysis of the gas phase, showing a peak at $m/z = 30$. On the basis of the ratio of the integrated intensity at the end of the process (Fig. 5b, curve 7) the fraction of ^{18}O exchanged CO, on the basis of the integrated intensities of the bands, is 0.3. However, it can be noticed that this "spectroscopic ratio" could be affected by an intensity transfer from the low frequency mode to the high frequency one through dipole–dipole interactions (6, 17). It could be then suggested that the actual $C^{16}O/C^{18}O$ is larger in amount.

In the 2400–2250 cm^{-1} range weak absorption bands due to the asymmetric stretching of the different isotopic CO_2 molecules formed in the reactions are observed: the multiplet of bands can be assigned to $C^{16}O_2$, $C^{16}O^{18}O$, and $C^{18}O_2$; the same species are also detected by quadrupole mass spectrometry.

The oxygen species involved in the oxidation and scrambling reactions could be atomic or molecular in principle, and any direct evidence about their nature was obtained by the experimental methods adopted. However, the spectroscopic features of CO–O_2 interactions observed in the present paper are very similar to those reported by Hollins and Pritchard on oxidised Cu(110), where a dissociative oxygen chemisorption occurred (17a).

Furthermore, many other experimental evidences, coming from different surface science techniques (19), indicate that, for instance, oxygen is dissociatively chemisorbed on the Cu(110) surface already at $T < 300$ K. Moreover, HREELS results supported by LEED, TPD, and STM data (19, 20) evidenced that the admission of O_2 on the Cu(100) plane produces highly reactive O^- species on defect sites, while less reactive O^{2-}-like species were associated with reconstructed Cu–O–Cu planes, clearly indicating that Cu sites in defect positions are more reactive than the nondefect ones and play a dominant role in sustaining the reaction. On very small, stepped metal particles a high concentration of isolated and uncoordinated Cu sites is expected, on which the reaction can occur easily. Our experimental data show IR evidences for a transient surface species in which CO and two oxygen atoms are bonded to the same metallic atom (bands at 2146 cm^{-1}) (Fig. 5a, curve 6). This species can be considered as a precursor of a carbonate species. This kind of intermediate was suggested by Schneider *et al.* (21) who studied CO oxidation on the Cu(110)–(2×1)–O surface. We recall here that CO

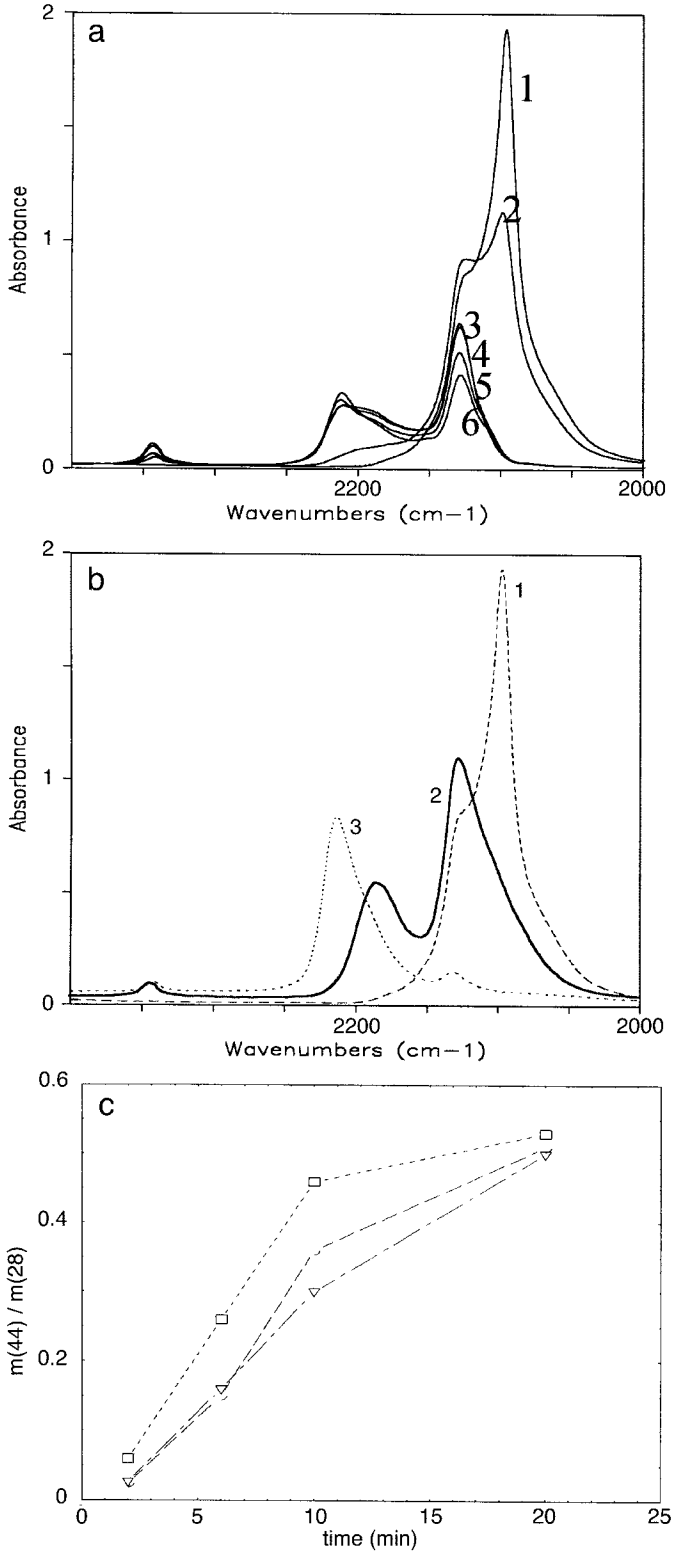

oxidation by O_2 adsorbed molecules was reported for Pt(111) (20) and Ag(110) (22) and, in those cases, surface carbonates were detected as intermediate species by HREELS.

We have shown that, in the presence of $^{18}O_2$, CO molecules exchange oxygen atoms to a large extent and the molecular integrity of CO is not preserved already at room temperature. It was shown that the surfaces of the copper metal crystallites in the methanol synthesis working catalysts are partially oxidised (23), and therefore we suggest that the scrambling of the oxygen atoms of adsorbed CO could actually occur also in the methanol synthesis conditions, while usually the molecular integrity of CO is assumed for this reaction. The chemisorption and the reactivity of CO on monocrystalline and supported metals has been extensively studied with different techniques (24). It is well known that carbon monoxide is weakly bonded on sp and d^{10} metals while the bond is strong and sometimes dissociative on transition metals. Looking at these features it is often proposed that d^{10} metals are selective in the hydrogenation of CO to form alcohol because they do not dissociate CO while the transition metals produce hydrocarbons because they do dissociate CO. However, the scrambling reaction in the mild conditions illustrated above indicates that probably the reasons for this different selectivity are more complex.

3.4.2. NO–CO interaction. The main point that we stress here is that the admission of NO at room temperature onto the catalysts does not produce bands in the 1900–1700 cm^{-1} range, where bands due to adsorbed NO are usually observed. By contrast, in spite of the absence of adsorbed NO molecules, reaction products of the CO–NO interaction are immediately evident: in the first few minutes of interaction at RT a band related to the reaction product CO_2 at 2350 cm^{-1} is produced (Fig. 6a, curves 1–6). Moreover, a broad absorption at 2180–2220 cm^{-1} appears; at the same time the band in the CO stretching region at 2128 cm^{-1} increases, while the bands at 2103 and 2071 cm^{-1} decrease in intensity. It can be stressed that the well-defined component at 2146 cm^{-1} detected during the interaction with oxygen is never observed during the CO–NO reaction experiments. As previously commented on, this behaviour suggests that the 2146 cm^{-1} band is related to a surface species produced by the reaction of CO with two oxygen atoms directly bonded to the same copper atom on which is adsorbed the carbon monoxide molecule, while this

FIG. 6. FTIR spectra of NO interaction with CO preadsorbed on Cu/Si reduced and outgassed at 523 K. (a) (1) Spectrum recorded in the presence of 10 mbar of CO; (2–6) spectra recorded after 2, 4, 6, 10, and 30 min, respectively, after the admission of 10 mbar NO onto preadsorbed CO. (b) Spectra recorded after (1) admission of 10 mbar CO of the freshly reduced Cu/Si sample (dashed line); (2) readmission of 10 mbar CO onto the sample outgassed at room temperature after the first CO–NO reaction run (solid line); (3) 30 min after the admission of 10 mbar NO onto preadsorbed CO (second CO–NO reaction run) (dotted curve). (c) $(m/z\ 44)/(m/z\ 30)$ versus reaction time determined during the 1° run (□), 2° run (o), 3° run (▽).

surface adduct is not produced by using NO as oxidant, as in this case essentially isolated oxygen atoms are produced by NO dissociation.

Immediately after the admission of NO on preadsorbed CO a small intensification of the band at 2128 cm^{-1} is observed (Fig. 6a, curves 1, 2), while after 30 min of contact the same band decreases its intensity (Fig. 6a, curve 6). At the same time modifications in the shape of the broad component at 2220–2180 cm^{-1} are observed. Absorption bands in this spectral region, irreversible to the outgassing at RT, produced by CO–NO interactions have been observed previously and have been assigned to the asymmetric stretching of isocyanate NCO species coordinated to oxidised or reduced copper sites or to isocyanate adsorbed on the support (25, 26). It has been shown by Solymosi and Bansagi (26) that NCO species formed by HCNO adsorption on different oxides exhibits NCO asymmetric stretch in the range 2300–2210 cm^{-1}, the frequency decreasing by decreasing the stability of the species. As for NCO species adsorbed on copper sites, the same authors assigned a band at 2230–2240 cm^{-1} to NCO on Cu(0), a band at 2200–2205 cm^{-1} to NCO on Cu(I), and a band at 2180–2185 cm^{-1} to NCO on Cu(II) sites. The absorption growing during CO–NO interaction in our case is initially located at 2180 cm^{-1} while after a long contact time the maximum is shifted at 2210 cm^{-1}. On the basis of the assignments reported above it could be proposed that at the beginning of the CO–NO interaction the NCO species are formed on Cu(II) centres, while during the reaction a modification of the adsorption sites into Cu(I) species probably occurs.

In Fig. 6b a comparison of the absorption spectrum produced by the first CO adsorption on a freshly reduced sample (curve 1), the spectrum obtained by readsorption of CO after outgassing at RT of a first reaction mixture (curve 2), and that obtained in a second CO–NO interaction (curve 3) is presented. It can be observed that in the spectrum of the readsorbed CO after the reaction (curve 2) the bands typical of CO adsorbed on 3D metallic particles are almost completely lacking. In the second run of the reaction the produced CO_2 appears weaker, and stronger bands are observed in the 2220–2150 cm^{-1} region (curve 3). From these data it appears evident that the catalytic activity of the samples remains high, almost unchanged, even when the microfacets of the 3D copper particles are covered by an oxidic layer, produced during the CO–NO interaction. However, some of the copper and support sites are already covered by isocyanate species produced by this process. Probably, the smaller intensity of the carbon dioxide absorption band detected by FTIR is due to the competitive coverage of the surface with isocyanate species, whose intensity increases during the successive interactions.

On the basis of these observations the almost constant activity of the samples in the successive interactions can be related to the presence of the isolated atoms or small 2D copper particles, slightly rendered electropositive by the interaction with the support. On these particles NO can be dissociate, producing highly reactive oxygen species, which are not incorporated to form a stable oxidic layer.

4. CONCLUSIONS

The characterisation of the Cu/SiO_2 and of the two Cu/SiO_2–TiO_2 catalysts by TEM, diffuse reflectance UV-Vis-NIR spectroscopy, and FTIR spectroscopy of adsorbed CO evidenced that the morphological and surface properties of the copper phase are essentially the same for all the systems investigated. In particular, all samples were found to contain both three-dimensional and plate-like two-dimensional metal particles. This clearly indicates that the features of the supported phase produced following the adopted preparation and activation methods do not depend on the nature of the carrier. This statement is confirmed by the fact that essentially the same types of supported particles were found in a Cu/TiO_2 catalyst prepared by the same method, the subject of previous studies.

Therefore, we could now plan to design a catalyst where the metal is suitably tailored and the support can exert its activity, if any, without influencing one another.

Interestingly, a fully reduced metal phase is obtained on all three samples already after treatment in H_2 in mild conditions (523 K). By reduction at higher temperature, the TiO_2 phase present in the systems supported on silica–titania forms TiO_x suboxides covering a fraction of the exposed Cu metal sites. This indicates that, even if present in low amount, the TiO_2 phase can interact in these conditions with the copper particles.

Information on the oxidative behaviour of the metal phase was obtained by studying the CO–O_2 and CO–NO reactions. The results obtained in the first case allow the conclusion that these systems are highly active towards O_2 and NO even at room temperature. Furthermore, the observed features indicated that the active sites in the CO–NO reaction are the Cu centres at the surface of two-dimensional particles.

ACKNOWLEDGMENT

The authors gratefully acknowledge financial support by Consiglio Nazionale delle Ricerche (CNR).

REFERENCES

1. Geus, J. W., and van Veen, J. A. R., *in* "Studies in Surface Science and Catalysis" (J. A. Moulijn, P. W. N. M. Leeuwen, and R. A. van Santen, Eds.), Vol. 79, p. 335. Elsevier, Amsterdam, 1993.
2. Schwarz, J. A., Contescu, C., and Contescu, A., *Chem. Rev.* **95**, 475 (1995).
3. Solomon, E. I., Jones, P. M., and May, J. A., *Chem. Rev.* **93**, 2623 (1993).

4. Boccuzzi, F., and Chiorino, A., *J. Phys. Chem*. **100**, 3617 (1996).
5. Boccuzzi, F., Guglielminotti, E., Martra, G., and Cerrato, G., *J. Catal.* **146**, 449 (1994).
6. Boccuzzi, F., Chiorino, A., Martra, G., Gargano, M., Ravasio, N., and Carrozzini, B., *J. Catal.* **65**, 129 (1997).
7. Boccuzzi, F., Chiorino, A., Gargano, M., and Ravasio, N., *J. Catal.* **165**, 140 (1997).
8. di Castro, V., Gargano, M., Ravasio, N., and Rossi, M., *in* "Studies in Surface Science and Catalysis" (G. Poncelet, P. A. Jacobs, P. Grange, and B. Delmon, Eds.), Vol. 63, p. 95. Elsevier, Amsterdam, 1991.
9. (a) Balkenende, A. R., van der Grift, C. J. G., Meulenkamp, E. A., and Geus, J. W., *Appl. Surf. Sci.* **68**, 161 (1993); (b) van der Grift, C. J. G., Elberse, P. A., Mulder, A., and Geus, J. W., *Appl. Catal.* **59**, 275 (1990).
10. Jernigan, G. G., and Somorjai, G. A., *J. Catal.* **147**, 567 (1994).
11. (a) Davis, R. J., and Liu, Z., *Chem. Mater.* **9**, 2311 (1997) and references therein; (b) Sheldon, R. A., and Van Doorn, J. A., *J. Catal.* **31**, 427 (1973); (c) Espinós, J. P., Lassaletta, G., Fernández, A., González-Elipe, A. R., Stampfl, A., Morant, C., and Sanz, J. M., *Langmuir* **14**, 4908 (1998).
12. Scholten, J. J. F., and Kovalinka, J. A., *Trans. Faraday. Soc.* **65**, 2456 (1969).
13. Vasilievich, A., Shpiro, G. P., Alekseev, A. M., Semenova, T. A., Markina, M. I., Vasil'eva, T. A., and Budkina, O. G., *Kinet. Katal.* **16**, 1363 (1975).
14. Osinga, T. J., Linsen, B. G., and van Beek, W. P., *J. Catal.* **7**, 277 (1967).
15. Vogel, R., Hoyer, P., and Weller, H., *J. Phys. Chem*. **98**, 3183 (1994).
16. Hummel, R. E., *Phy. Stat. Sol. A* **76**, 11 (1983).
17. (a) Hollins, P., and Pritchard, J., *Surf. Sci.* **134**, 91 (1983); (b) Hollins, P., *Surf. Sci. Rep.* **16**, 51 (1992).
18. Campbell, C. T., *Surf. Sci. Rep.* **27**, 1 (1997).
19. (a) Sasaki, T., Sueyoshi, T., and Iwasawa, Y., *Surf. Sci.* **316**, L1081 (1994); (b) Sueyoshi, T., Sasaki, T., and Iwasawa, Y., *J. Phys. Chem*. **100**, 1048 (1996).
20. Crew, W. W., and Madix, R. J., *Surf. Sci.* **319**, L34 (1994).
21. Schneider, T., and Hirschwald, W., *Catal. Lett.* **16**, 335 (1992).
22. Matsushima, T., *Surf. Sci.* **127**, 403 (1983).
23. Capote, A. J., Roberts, J. T., and Madix, R. J., *Surf. Sci.* **209**, L151 (1989).
24. Fu, S. S., and Somorjai, G. A., *J. Phys. Chem*. **96**, 4542 (1992), and references therein.
25. Solymosi, F., Volgyesi, L., and Sarkany, J., *J. Catal.* **54**, 336 (1978).
26. Solymosi, F., and Bansagi, T., *J. Catal.* **156**, 75 (1995).